

CT-based Analysis of Vascular Tree Abnormalities in Different Phenotypes of COVID-19 Pneumonia

Gihad Ibrahim ^{a,*}, Ahmed Hassan ^b

^a Department of Biomedical Engineering, Mashreq University, Khartoum North, Sudan

^b Department of Telecommunication Engineering, Mashreq University, Khartoum North, Sudan

Corresponding author: *gibrahim@mashreq.edu.sd

Abstract— In this paper, Computed Tomography (CT) images of six confirmed COVID-19 patients were analyzed in order to investigate the physiological abnormalities in the vascular tree in response to the disease-induced hypoxia. The CT images were classified into an L-type and H-type groups based on the cumulative voxel distribution of the CT scan. A 3-Dimensional model of the vascular tree was reconstructed out of each CT image following a computational framework. Then, the Cross-Sectional Area (CSA) of the vessels belonging to each vascular tree was computed. The acquired results were compared against averaged measurements of three healthy subjects that were computed following the same approach. The results showed that as the severity of COVID-19 lean towards H-type phenotype, signs of vasoconstriction in small blood vessels with a CSA less than 10 mm² tend to decrease, whereas signs of vasodilation in medium to large blood vessels increases. The intensity of dilated blood vessels proximal to consolidated areas of the lung was found to increase significantly as the disease progresses in the lungs. Furthermore, signs of vasoconstriction and vasodilation in the vascular tree were observed in all lobes of the lung in both phenotypes including seemingly healthy lobes. The results in this paper are suggestive of intrapulmonary blood flow shunting towards unaerated areas of the lungs which may lead to a ventilation/perfusion mismatch even at minor cases of COVID-19. The results also suggest that subject-specific regulated use of vasodilating medication may reduce the number of cases that require mechanical ventilation.

Keywords— COVID-19 pneumonia; SARS-CoV-2; COVID-19 phenotypes; vascular tree analysis.

Manuscript received 19 Jul. 2020; revised 18 Feb. 2021; accepted 20 Apr. 2021. Date of publication 30 Jun. 2022.
IJASEIT is licensed under a Creative Commons Attribution-Share Alike 4.0 International License.



I. INTRODUCTION

Coronavirus disease 2019 (COVID-19) is the outbreak of pneumonia caused by a novel coronavirus officially named the severe acute respiratory syndrome coronavirus 2 (SARS-CoV-2) [1]. This virus was initially discovered in Wuhan, Hubei province, China, in December 2019 [2]. It seems to be a very contagious virus that has rapidly spread globally, causing a significant global health pandemic [3]. By mid-July 2020, data from the World Health Organization (WHO) reveal that more than thirteen million people worldwide are diagnosed with the disease, and the fatality rate has exceeded the 4.3 % margin.

Although this disease satisfies the 2012 Berlin Definition of Acute Respiratory Distress Syndrome (ARDS) [4], many emerging studies suggest that COVID-19 has its unique and peculiar phenotypes requiring further investigation. Severe hypoxic respiratory failure is the main feature of this disease. However, what characterizes it from a typical ARDS is that,

in several cases, the resultant pulmonary hypoxia is associated with near-normal respiratory system compliance [5]–[8]. Such an interesting combination of characteristics indicates that alveolar damage may not be the main cause of the hypoxic respiratory failure seen in some COVID-19 patients. In contrast, many studies suggest that the formation of pulmonary microvascular thrombosis, as an inflammatory reaction following the alveolar viral damage, could be the main reason behind the high number of deaths by COVID-19 [9]–[12].

Gattinoni *et al.* [5] hypothesized that COVID-19 patients could be classified into two main categories (phenotypes), the L-type and the H-type patients. The L-type COVID-19 is usually seen at the early stages of the disease, where lung compliance is almost normal. Nonetheless, low ventilation to perfusion (V_A/Q) ratio with low lung weight is often observed in those patients, indicating that a dysfunction of the blood supply induces the respiratory hypoxia in L-type COVID-19 to the oxygenated alveoli rather than alveolar damage. Conversely, in the H-type patients, inflammatory exudate

builds up inside the alveoli, along with the thickening of the alveolar and the vascular wall is observed. This is accompanied by a high lung elastance, a typical scenario of severe ARDS [13]. Thus, those two types of COVID-19 phenotypes may occur separately, or they may progress from one type to another. It is, therefore, extremely essential to improve our understanding of the differences in the pathophysiology between those two phenotypes for enhanced treatment and better mechanical ventilation management protocols.

It is generally believed that, in common bacterial and viral pneumonia patients, two types of lung vascular abnormalities are observed. Initially, the body's immune system expands (vasodilates) the vascular blood vessels near the infected alveoli to increase the vascular permeability to those areas, which may eventually lead to alveolar edema and proteinosis [14]. When the body detects severe alveolar hypoxia, the lung attempts to physiologically redirect the unoxygenated blood in the arteries to better-aerated alveoli to optimize the V_A/Q ratio. This is done by constricting the small intrapulmonary arteries near the hypoxic alveoli, which causes an increase in resistance to the blood flowing towards those areas in a physiological phenomenon known as hypoxic pulmonary vasoconstriction (HPV) [15].

The reported vascular abnormality response in COVID-19 patients is also not consistent with that of a typical ARDS. For example, Lang *et al.* [16] noticed in dual-energy CT scans of 12 COVID-19 patients severe perfusion abnormalities caused by blood shunting toward areas where gas exchange is impaired due to vasodilating the blood vessels predominately within, or surrounding, areas of lung opacities. Furthermore, an autopsy study performed by Tian *et al.* [17] also observed severe vascular congestion in early-phase COVID-19 patients. In addition, an ongoing study involving more than 500 COVID-19 patients performed by the functional respiratory imaging (FRI) company Fluidra [18] showed that the virus is resulting in severe vasoconstriction of small capillaries in the lung, and vasodilators delivered to the lung is a recommended therapy. However, studies like [6], [7], [19] suggest that loss of hypoxic pulmonary vasoconstriction is the main cause of impaired regulation of pulmonary blood flow in L-type patients of COVID-19, which results in the severe V_A/Q mismatch. Thus, the physiological vascular abnormality response to COVID-19 is controversial and requires further investigation.

In this paper, CT scans of confirmed L-type and H-type COVID-19 patients are used to analyze the physiological vascular tree abnormality response to the disease compared to those of healthy subjects. The contribution of this paper is that it enhances our understanding of the physiological differences between the two main types of COVID-19 pneumonia. Furthermore, it provides an estimate of the physiological abnormality response to the virus in the vascular tree at different severity stages of the disease, which may improve the clinical management of patients at the hospitals.

II. MATERIAL AND METHODS.

A. Analysis of Vascular Abnormalities Overview

Mashreq University Research Ethics Committee approved this study. Fig 1 illustrates a flowchart of the main steps

adopted to analyze the vascular abnormalities caused in response to COVID-19 infection. The approach utilizes data from thoracic CT images of healthy and diseased subjects. The CT images of the COVID-19 subjects are classified into L-type and H-type subject groups based on the cumulative voxel distribution of the CT scan. Then, an image processing approach was implemented for the segmentation and the 3-Dimensional (3D) reconstruction of the vascular tree out of each CT image. The cross-sectional area (CSA) of the generated blood vessels is then computed as the sectional surface area normal to the blood vessel centerline.

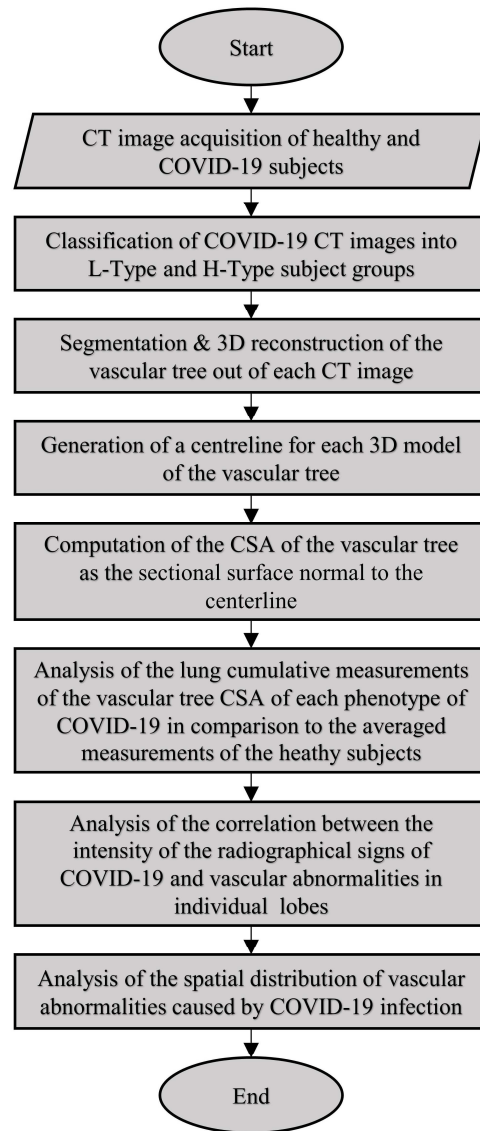


Fig. 1 The general approach adopted to analyze the vascular tree abnormalities caused by COVID-19 phenotypes.

The analysis of the acquired results was performed in three main stages. Firstly, the cumulative measurements of the cross-sectional area of the pulmonary blood vessels of the entire lung acquired from the L-type and H-type COVID-19 subject groups were evaluated concerning the averaged measurements of the healthy subject group. Then, the changes in CSA of the blood vessels within the individual lobes because of COVID-19 infection was analyzed. This was done to evaluate the correlation between the intensity distribution

of COVID-19 radiographical signs on CT images and the vascular abnormality caused in response to each phenotype of the disease. Finally, the spatial distribution of the CSA of the blood vessel surrounding the opacities and consolidation caused by COVID-19 in each subject group was analyzed to evaluate the phenomena of intrapulmonary blood flow shunting towards areas of the lung where gas exchange is reduced, causing ventilation/perfusion mismatch.

B. CT Scans Acquisition

Nine CT images are used in this study. Six of which are confirmed positive COVID-19 patients obtained from the public datasets available at [20]. The remaining three CT images were acquired from healthy subjects with no known history of smoking or chronic pulmonary disease. Table 1 outlines the general information of each CT image along with its acquisition parameters. As shown in Fig. 2, the CT images of the COVID-19 patients were classified into L-type and H-type COVID-19 groups based on the cumulative voxel distribution of the CT scan as described in [5].

TABLE I
CT IMAGES PARAMETERS

| Case ID | Gender | Pixel Size (mm) | KVP | Slice Thickness (mm) | Pitch |
|--------------------------|--------|-----------------|-----|----------------------|-------|
| COVID-19 (L-Type) | | | | | |
| CL-1 | Male | 0.69 | 120 | 1 | 1.125 |
| CL-2 | Male | 0.69 | 120 | 1 | 1.25 |
| CL-3 | Male | 0.76 | 120 | 1.5 | 1.075 |
| COVID-19 (H-Type) | | | | | |
| CH-1 | Male | 0.68 | 120 | 1 | 1.075 |
| CH-2 | Male | 0.68 | 120 | 1.5 | 1.075 |
| CH-3 | Male | 0.74 | 120 | 1.5 | 1.075 |
| Non-COVID-19 | | | | | |
| H-1 | Male | 0.68 | 120 | 1.25 | 1.075 |
| H-2 | Male | 0.64 | 120 | 1.25 | 1.075 |
| H-3 | Male | 0.64 | 120 | 1.25 | 1.075 |

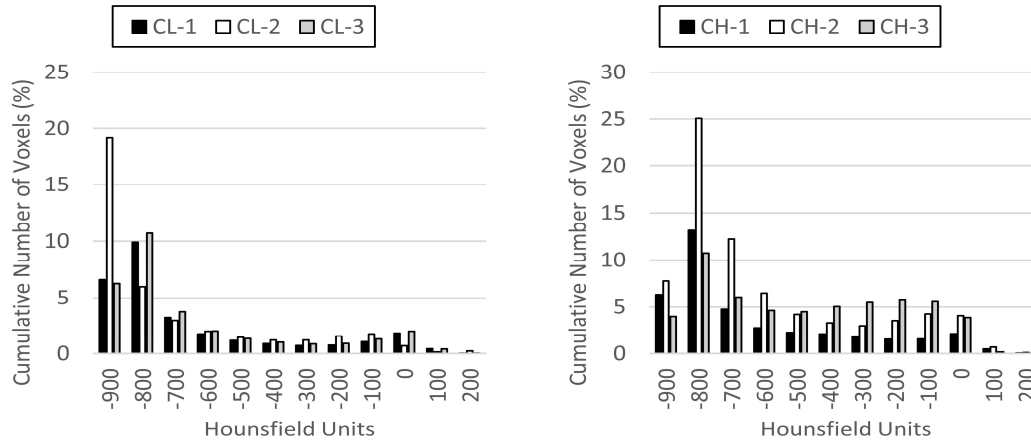


Fig. 2 The cumulative distribution of the Hounsfield units of the CT images of the L-type (left) and H-Type (right) patients

As a result, each COVID-19 group contained three CT images labeled from 1 to 3 based on the severity of the observed radiographical signs of the disease, where case CL-3 and case CH-3 are the most severely affected cases the L-type and the H-type group, respectively.

It is important to note that CT imaging of COVID-19 patients illustrates some spatial radiographical signs of the disease, including, but not limited to, Ground Glass Opacities (GGOs) sometimes associated with air space consolidation [21]–[23]. However, similar features are also seen in CT scans of typical pneumonia patients, and hence, CT scanning is not recommended to be used for the diagnosis of COVID-19 [24].

C. Computation of the Blood Vessels Cross-Sectional Area

Fig. 3 illustrates the main steps adopted to compute the vascular tree's Cross-Sectional Area (CSA) in each case. First, a 3-Dimensional (3D) model of the pulmonary vascular tree was reconstructed out of each CT image dataset following the methodology described in [25]. Briefly, a Gaussian 3D filter (radius =1) was applied to the image slices using the open-source software ImageJ (NIH, Bethesda, Maryland, USA) in order to reduce the noise in the images (Fig. 3(a)). Then, a 3D mask of the lung parenchyma was generated by inserting a

seed within the lung volume using the 3D Toolkit in ImageJ (Fig. 3(b)). The 3D Dilate and the 3D Erode functions, also available within the 3D toolkit of ImageJ, were then applied to the generated masks to fill the missing voxels and smooth the boundaries. The generated lung masks were then added to their originating images using the image calculator tool in ImageJ (Fig. 3(c)).

Furthermore, an enhanced contrast function was applied for better segmentation results. Finally, the tubeless filter [26] was applied to the processed images in order to extract the pulmonary vascular tree from its surroundings by examining the connectivity between the pixels within the images dataset based on the eigenvalues of the Hessian matrix (Fig. 3(d)). The resulting images were then imported into the open-source medical image processing software 3D Slicer V4.10.2 for the 3D reconstruction process of the vascular tree (Fig. 3(e)).

The generated 3D models were cleaned up manually to remove any leakage resulting from image blurring or the presence of consolidation due to the viral infection in the CT images of the COVID-19 patients. The blood vessels belonging to each lung lobe were then, separated and a centerline was generated for each set of blood vessels, as shown in Fig. 3(f). Finally, the CSA was computed as the

sectional surface area normal to the points constructing the generated centerline of the vascular tree.

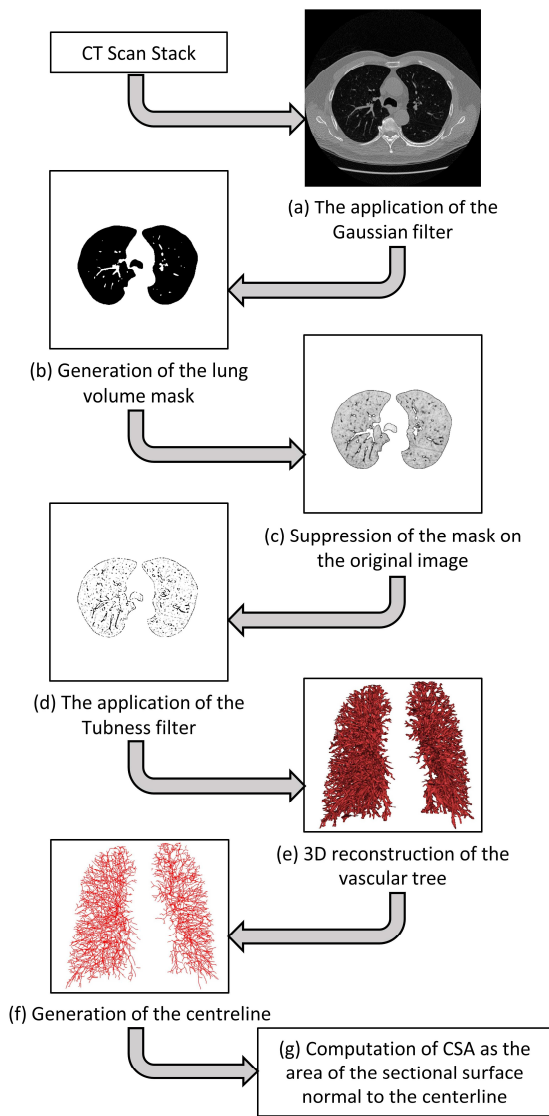


Fig. 3 The computational framework to estimate the Cross-Sectional Area (CSA) of the vascular tree.

III. RESULTS AND DISCUSSION

A. Analysis of the Total Lung Vascular Tree

The cumulative distribution of the CSA of the vascular tree acquired from the CT images of the COVID-19 patients was compared to the averaged value of those of the healthy patients as shown in Fig. 4. The averaged values of the CSA of the healthy subjects were computed with a correlation coefficient of 0.98 ± 0.01 . It can be noticed clearly that in all types of COVID-19 cases, the highest discrepancies are observed in the small blood vessels with a CSA of 10 mm^2 or less. However, medium to large blood vessels is affected significantly only in H-type cases.

An increase of up to 11.5% in the volume of the blood vessels with a CSA less than five mm^2 was observed in L-type patients. This is a sign of severe vasoconstriction in such small blood vessels. As the severity of COVID-19 leans towards the H-type phenotype, signs of vasoconstriction in such small blood vessels seem to decrease. In the most severe

L-type case (CL-3), the volume of the small blood vessels with a CSA less than 5 mm^2 decreased by 30%, whereas the volume of the blood vessels with a CSA range of $5\text{-}10 \text{ mm}^2$ increased by 4.7%. Similar observations can be made in the results of the least severe H-type patient (CH-1). This is a significant indicator of a severe mismatch in the blood vessels' cross-sectional area, which may cause blood flow shunting. In intermediate to severe H-type patients, the volume of the small blood vessels with a CSA less than 10 mm^2 decreased by 13-30%, whereas an increase of up to 33.5% was observed in the volume of the blood vessels with a CSA larger than 20 mm^2 in those cases.

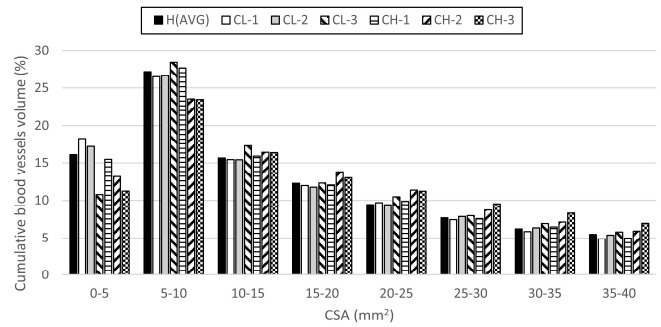


Fig. 4 The cumulative measurements of the cross-sectional area of the pulmonary blood vessels acquired from the L-type and H-type COVID-19 patients in comparison to the averaged measurements of the healthy subjects.

It could be clearly seen from Fig 4 that the CSA of the small and large blood vessels are severely affected in COVID-19. No signs of significant vasodilation were observed in minor to intermediate cases of L-type patients. However, signs of severe vasoconstriction in small blood vessels in the same subject group were present. In contrast, signs of severe vasodilation were observed in H-type patients, whereas the results of the same subject group showed no signs of severe vasoconstriction. In transitional cases (i.e., cases that could be classified as either L-type or H-type) a significant mismatch in the small blood vessels with a CSA less than 10 mm^2 was observed.

B. Analysis of the Vascular Tree of Individual Lobes

1) *L-Type Patients:* Similar to the common types of pneumonia, COVID-19 infection may affect a single lobe, or it may spread throughout the lung tissue. All L-type cases examined in this study were found to be single lobe infected patients, where ground-glass opacities (GGOs) were observed in a single lobe, and the other pulmonary lobes did not illustrate any radiographical signs of COVID-19. Nonetheless, significant discrepancies were observed in the CSA measurements of the blood vessels belonging to those seemingly uninfected lobes compared to the averaged measurements of the blood vessels of the healthy subjects. For example, signs of GGOs and consolidation were observed only at the Left Lower Lobe (LLL) of Case CL-1. However, the volume of the blood vessels with a CSA less than 5 mm^2 was increased by 20.4% at the Right Lower Lobe (RLL) of CL-1, as shown in Fig 5. indicating severe vasoconstriction within that seemingly healthy lobe. Although not significant, signs of vasodilation were also not limited to the infected lobes. Similar observations could be made on the results of

case CL-2 and CL-3. Only the Right Lower Lobe (RLL) seems to be infected in those two cases. Nevertheless, significant discrepancies can be seen in the CSA

measurements of the blood vessels belonging to all lobes of the lung compared to the healthy subject reference measurements.

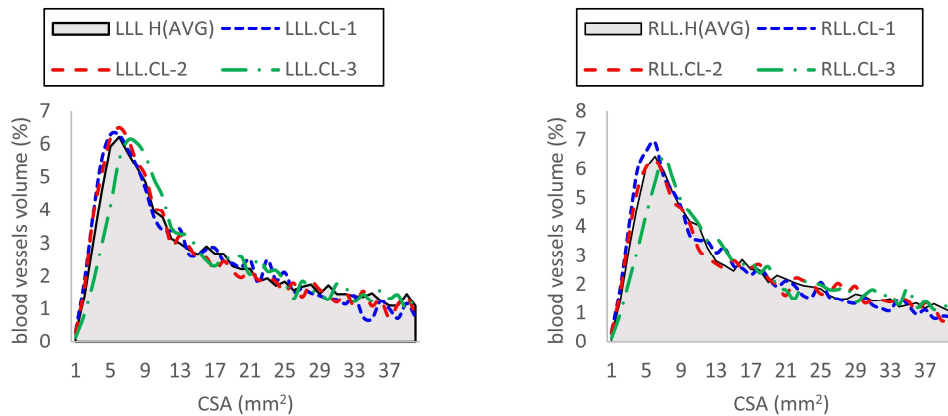


Fig. 5 Measurements of the Cross-Sectional Area (CSA) of the blood vessels within the Left Lower Lobe (LLL) and the Right Lower Lobe (RLL) of the L-type COVID-19 patients in comparison to the averaged measurements of the healthy subjects.

Therefore, the results indicate that, even though a single lobe might be infected by COVID-19 pneumonia, signs of vasoconstriction and vasodilation are present in other uninfected lobes. This might also cause a blood flow shunting towards less oxygenated tissues that lead to severe hypoxia even though radiographical signs of COVID-19 are less present in such types of cases. The results also suggest that signs of vasoconstriction decrease, and signs of vasodilation increases as the diseases progresses in the lungs

2) *H-Type* Patients: All H-type subjects examined in this study showed radiographical signs of COVID-19 distributed

on all the pulmonary lobes. However, some lung zones were more infected than others. For example, the CT images of case CH-1 showed more predominant signs of COVID-19 at the upper and middle lung zones. Nonetheless, signs of vascular abnormalities were observed on the CSA measurements of the blood vessels belonging to the five lobes. However, similar to L-type patients, the results of the lower lobes showed more vascular abnormalities compared to the upper lobes of the lungs, as shown in Fig. 6.

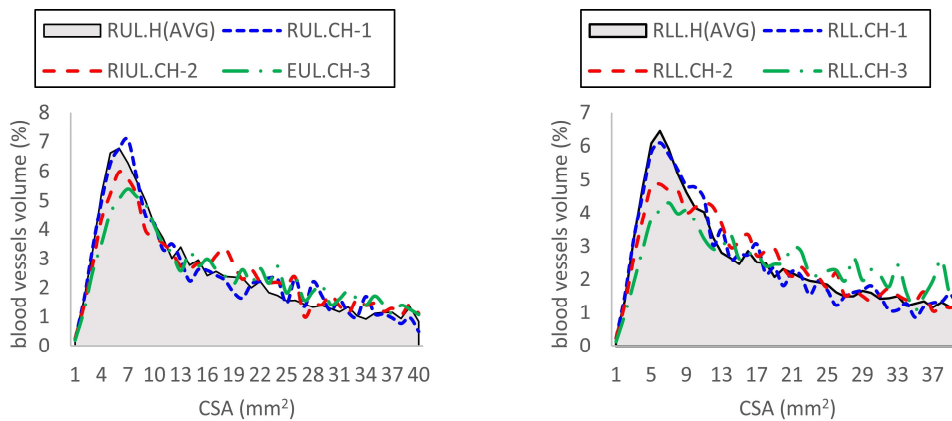


Fig. 6 Measurements of the Cross-Sectional Area (CSA) of the blood vessels within the Left Lower Lobe (LLL) and the Right Lower Lobe (RLL) of the L-type COVID-19 patients in comparison to the averaged measurements of the healthy subjects.

Additionally, it is interesting to note that the volume of the blood vessels with a CSA less than 5 mm² decreases as the signs of COVID-19 increase in this type of patient. This indicates that vasoconstriction may not be as intense in H-type COVID-19 patients as in the L-type patients. However, signs of vasodilation are more prominent in H-type patients' results than the L-type ones, and such signs increase as the severity of the infection intensifies in the lung. This is mainly due to the physiological inflammatory response of the lung to the

viral infection. Thus, blood flow shunting towards unoxygenated areas of the lung is also present in the H-type COVID-19 patients

C. *Spatial Distribution of Vascular Abnormalities*

Fig 7 illustrates the spatial distribution of the CSA of the blood vessel surrounding the opacities and consolidation caused by COVID-19 in a sagittal view. The illustrated results were acquired from cases CL-1, CH-1, and CH-3. It could be

seen that the blood vessels tend to dilate proximal to lung opacity and consolidation. The intensity of such vasodilation increases dramatically as the area of the lung opacity and consolidation increases. On the other hand, signs of vasoconstriction proximal to lung opacity and consolidation were less observed in the results of CH-1 and CH-3 compared to that of CL-1, whereas the intensity of the small blood vessels (CSA $< 5 \text{ mm}^2$) peripheral to the area of lung opacity and consolidation seems to decrease as the diseases progress in the lungs. This indicates that the lung physiological hypoxic vasoconstriction response tends to be dysfunctional in severe COVID-19 cases.

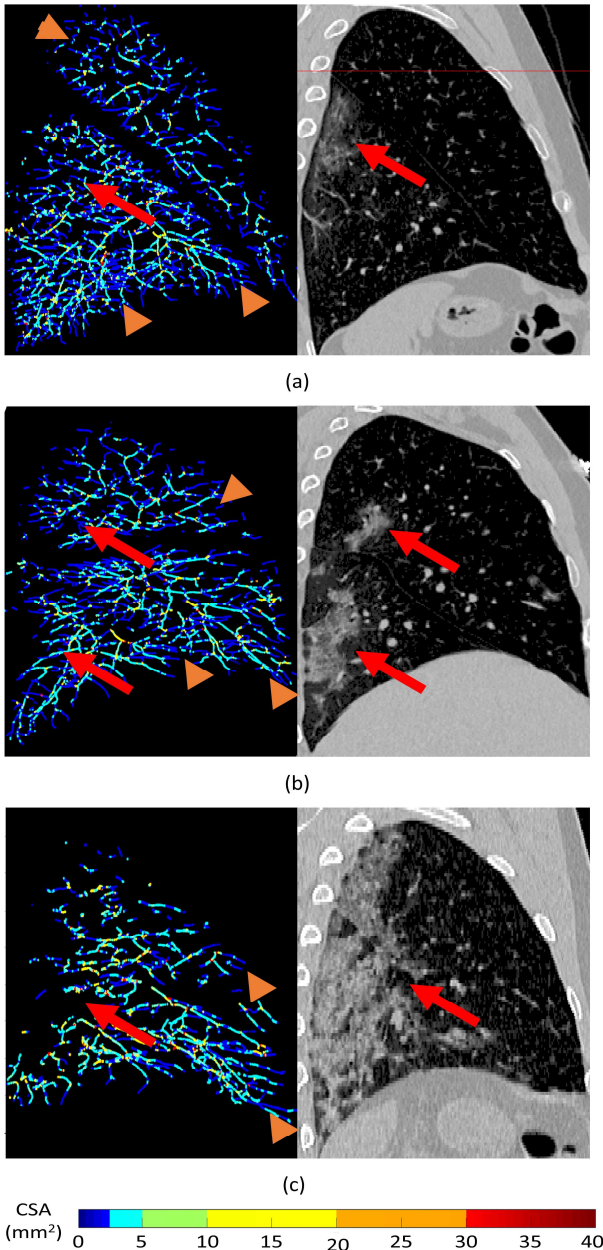


Fig. 7 Spatial visualization of vascular abnormalities in COVID-19 patients. (a) Case CL-1, (b) Case CH-1, and (c) Case CH-3. The long red arrows indicate the corresponding spatial location of COVID-19 radiographical signs. Orange arrowheads indicate small blood

Furthermore, the observed differences in blood vessels cross-sectional area surrounding the opacities and consolidation increase intrapulmonary blood flow shunting

towards areas of the lung where gas exchange is reduced, causing ventilation/perfusion mismatch even at minor cases of COVID-19. Therefore, vasodilator medications at early stages of COVID-19 pneumonia might reduce the number of patients requiring mechanical ventilation.

D. Study Limitations

The results shown in this study indicate that small blood vessels with a CSA less than 5 mm^2 experience significant vasoconstriction, particularly at L-type patients. However, the presented results are limited by the relatively low CT image resolution, which does not allow the 3D reconstruction and analysis of the small blood vessels (arteries and veins) with a CSA less than the CT image pixel size ($0.64 - 0.76 \text{ mm}^2$). Such volume of small blood vessels is estimated to represent more than 5% of the total volume of the vascular tree in healthy subjects [27]. Therefore, an imaging modality with a higher resolution, such as dual-CT, may provide more refined results of vascular tree abnormalities in COVID-19. In addition, areas of opacities and consolidation in CT images may prevent the 3D reconstruction of the blood vessels located within. Therefore, the presented results are not a precise representation of the true volume of the vascular tree. Finally, although the examined subjects represent various severity cases of COVID-19, the number of the examined subjects has to increase in future studies for more reliable outcomes.

IV. CONCLUSION

Despite sharing the same etiology (SARS-CoV-2), the physiological response to COVID-19 infection may differ dramatically from one patient to another. The findings in this study are strong indications that COVID-19 infection causes dysfunction to the physiological vascular abnormality response to typical hypoxia. However, such dysfunction may vary depending on the phenotype of the disease. In L-type COVID-19 patients, where lung compliance is almost normal, the blood vessel proximal to consolidated areas of the lungs were vasodilated, whereas signs of vasoconstriction were observed in small blood vessels of other seemingly healthy zones of the lung. Such vascular abnormalities may cause pressure difference, which leads to a blood flow shunting towards tissues of the lung where gas exchange is impaired. This explains the reason behind the ventilation/perfusion mismatch that may occur even in minor cases of COVID-19. In H-type patients, the edema tends to build up, and lung gas volume decreases as in a typical ARDS infection. Although signs of vasoconstriction were less present in this subject group, signs of vasodilation were significantly prominent, and the intensity of such signs increases as the severity of the edema intensifies in the lungs. This configuration abnormality in the vascular tree will also superimpose a pressure difference that causes blood flow shunting towards less oxygenated tissues of the lungs.

Although the number of the investigated subjects is small, the vascular abnormality response to COVID-19 was found to be subject-specific depending on the severity of the infection. Hence, it may not be sufficient to classify the disease spectrum into two main broad phenotypes for treatment and mechanical ventilation protocols. The results in this study also

support the hypothesis that using vasodilated medications at early stages may improve the ventilation/perfusion ratio and, hence, reduce the number of patients requiring ICU admission.

REFERENCES

- [1] C.-C. Lai, T.-P. Shih, W.-C. Ko, H.-J. Tang, and P.-R. Hsueh, "Severe acute respiratory syndrome coronavirus 2 (SARS-CoV-2) and corona virus disease-2019 (COVID-19): the epidemic and the challenges," *Int. J. Antimicrob. Agents*, vol. 55, no. 3, p. 105924, 2020.
- [2] D. Wang *et al.*, "Clinical characteristics of 138 hospitalized patients with 2019 novel coronavirus-infected pneumonia in Wuhan, China," *Jama*, vol. 323, no. 11, pp. 1061–1069, 2020.
- [3] C. Sohrabi *et al.*, "World Health Organization declares global emergency: A review of the 2019 novel coronavirus (COVID-19)," *Int. J. Surg.*, vol. 76, pp. 71–76, 2020.
- [4] A. D. T. Force, V. M. Ranieri, G. D. Rubenfeld, B. T. Thompson, N. D. Ferguson, and E. Caldwell, "Acute respiratory distress syndrome," *Jama*, vol. 307, no. 23, pp. 2526–2533, 2012.
- [5] L. Gattinoni *et al.*, "COVID-19 pneumonia: different respiratory treatments for different phenotypes?," *Intensive Care Med.*, vol. 46, pp. 1099–1102, 2020.
- [6] L. Gattinoni, D. Chiumello, and S. Rossi, "COVID-19 pneumonia: ARDS or not?," *Crit. Care*, vol. 24, no. 1, p. 154, 2020, doi: 10.1186/s13054-020-02880-z.
- [7] L. Gattinoni, S. Coppola, M. Cressoni, M. Busana, S. Rossi, and D. Chiumello, "Covid-19 does not lead to a 'typical' acute respiratory distress syndrome," *Am. J. Respir. Crit. Care Med.*, vol. 201, no. 10, pp. 1299–1300, 2020.
- [8] J. Wang *et al.*, "Tissue plasminogen activator (tPA) treatment for COVID-19 associated acute respiratory distress syndrome (ARDS): a case series," *J. Thromb. Haemost.*, vol. 8, no. 7, pp. 1752–1755, 2020.
- [9] F. Ciceri *et al.*, "Microvascular COVID-19 lung vessels obstructive thromboinflammatory syndrome (MicroCLOTS): an atypical acute respiratory distress syndrome working hypothesis," *Crit Care Resusc.*, vol. 22, no. 2, pp. 95–97, 2020.
- [10] F. A. Klok *et al.*, "Incidence of thrombotic complications in critically ill ICU patients with COVID-19," *Thromb. Res.*, vol. 191, pp. 145–147, 2020.
- [11] F. Zhou *et al.*, "Clinical course and risk factors for mortality of adult inpatients with COVID-19 in Wuhan, China: a retrospective cohort study," *Lancet*, vol. 395, no. 10229, pp. 1054–1062, 2020.
- [12] H. Bösmüller *et al.*, "The evolution of pulmonary pathology in fatal COVID-19 disease: an autopsy study with clinical correlation," *Virchows Arch.*, vol. 477, no. 3, pp. 349–357, 2020.
- [13] L. Gattinoni, T. Tonetti, and M. Quintel, "Regional physiology of ARDS," *Crit. Care*, vol. 21, no. 3, pp. 9–14, 2017.
- [14] D. R. Thickett, L. Armstrong, S. J. Christie, and A. B. Millar, "Vascular endothelial growth factor may contribute to increased vascular permeability in acute respiratory distress syndrome," *Am. J. Respir. Crit. Care Med.*, vol. 164, no. 9, pp. 1601–1605, 2001.
- [15] K. J. Dunham-Snary *et al.*, "Hypoxic pulmonary vasoconstriction: from molecular mechanisms to medicine," *Chest*, vol. 151, no. 1, pp. 181–192, 2017.
- [16] M. Lang *et al.*, "Hypoxaemia related to COVID-19: vascular and perfusion abnormalities on dual-energy CT," *Lancet Infect. Dis.*, vol. 20, pp. 1365–1366, 2020.
- [17] S. Tian, W. Hu, L. Niu, H. Liu, H. Xu, and S.-Y. Xiao, "Pulmonary pathology of early phase 2019 novel coronavirus (COVID-19) pneumonia in two patients with lung cancer," *J. Thorac. Oncol.*, vol. 15, no. 5, pp. 700–704, 2020.
- [18] FLUIDDA, "Our War on COVID-19," 2020. <https://www.fluidda.com/covid19/> (accessed May 25, 2020).
- [19] J. J. Marini and L. Gattinoni, "Management of COVID-19 respiratory distress," *Jama*, vol. 323, no. 22, pp. 2329–2330, 2020, doi: 10.1001/jama.2020.6825.
- [20] D. A. Paiva, "Coronacases.org: the first initiative of publicly deploy whole CT scans of covid-19 [CT Datasets]," 2020. <https://coronacases.org/> (accessed May 25, 2020).
- [21] H. Y. F. Wong *et al.*, "Frequency and distribution of chest radiographic findings in COVID-19 positive patients," *Radiology*, p. 201160, 2020.
- [22] F. Pan *et al.*, "Time course of lung changes on chest CT during recovery from 2019 novel coronavirus (COVID-19) pneumonia," *Radiology*, vol. 295, pp. 715–721, 2020.
- [23] H. Shi *et al.*, "Radiological findings from 81 patients with COVID-19 pneumonia in Wuhan, China: a descriptive study," *Lancet Infect. Dis.*, vol. 20, no. 4, pp. 425–434, 2020.
- [24] S. Kooraki, M. Hosseiny, L. Myers, and A. Gholamrezanezhad, "Coronavirus (COVID-19) outbreak: what the department of radiology should know," *J. Am. Coll. Radiol.*, vol. 17, no. 4, 2020.
- [25] G. Ibrahim, A. Rona, and S. V. Hainsworth, "Non-uniform central airways ventilation model based on vascular segmentation," *Comput. Biol. Med.*, vol. 65, pp. 137–145, 2015.
- [26] Y. Sato *et al.*, "Three-dimensional multi-scale line filter for segmentation and visualization of curvilinear structures in medical images," *Med. Image Anal.*, vol. 2, no. 2, pp. 143–168, 1998.
- [27] W. Huang, R. T. Yen, M. McLaurine, and G. Bledsoe, "Morphometry of the human pulmonary vasculature," *J. Appl. Physiol.*, vol. 81, no. 5, pp. 2123–2133, 1996.